

Supplement of *Clim. Past*, 10, 1905–1924, 2014  
<http://www.clim-past.net/10/1905/2014/>  
doi:10.5194/cp-10-1905-2014-supplement  
© Author(s) 2014. CC Attribution 3.0 License.



*Supplement of*

## **Fire in ice: two millennia of boreal forest fire history from the Greenland NEEM ice core**

**P. Zennaro et al.**

*Correspondence to:* P. Zennaro (piero@unive.it)

## SUPPLEMENTARY DATA

### **Levoglucosan Analyses: Materials, reagents and instrumentation**

All pre-analytical steps including decontamination of LDPE bottles, vials and sample bags were performed under a Class-100 clean bench located in a Class-10,000 clean room at the University of Venice. Sampling procedures were optimized to analyze trace elements and levoglucosan on the same samples. In order to minimize interference for trace element analysis the storage bottles were subject to strict decontamination procedures. Suprapur grade HNO<sub>3</sub> (65%, Merck) was used for all cleaning. We used a Purelab Ultra system (Elga, High Wycombe, U.K.) to produce the ultrapure water (18.2 MΩ cm, 0.01 TOC) utilized in all the analytical and pre-analytical procedures (i.e. cleaning and decontamination procedures, standard solution preparation) (Barbante et al., 1999; Gambaro et al., 2008)

All bottles were left for one week in each of the 3 subsequent solutions (5%, 2% and 1%) of HNO<sub>3</sub> and ultrapure water. The bottles were rinsed 3 times with ultrapure water between each bath. Bottles were stored filled with water in three layers of pre-cleaned polyethylene plastic bags. These cleaned LDPE 15 mL-bottles (Nalgene Corporation, Rochester, NY) were sent to the NEEM camp to store the collected melted ice samples. LDPE bottles used to contain the levoglucosan standard solutions and the polyethylene vials (Agilent Technologies, Wilmington, DE) for the chromatographic analysis were washed in ultrapure water, sonicated in an ultrasonic bath with ultrapure water (3 times for 14 minutes each) and rinsed with water. The cleaned bottles and vials were stored filled with water in pre-cleaned LDPE bags and were rinsed again with ultrapure water before using.

Samples and standards were transferred using Eppendorf pipettes and polyethylene tips (Eppendorf AG, Hamburg, Germany). The levoglucosan standard (purity of 99.7%) used for response factors was obtained from Sigma-Aldrich (Steinheim, Germany). Labeled levoglucosan (<sup>13</sup>C<sub>6</sub> enriched to 98%, purity of 98%) was purchased from Cambridge Isotope Laboratories Inc. (Andover, MA). Standard solutions were prepared through successive dilutions with ultrapure water. Standard solutions were stored at +4 °C in pre-cleaned PE bags until the sample preparation. HPLC/MS - grade methanol was purchased from Romil Ltd. (Cambridge, U.K.). Ammonium hydroxide (≥ 25%) analytical grade was purchased from Sigma-Aldrich (Steinheim, Germany). The 13 mM ammonium hydroxide solutions were prepared by adding ultrapure water.

We used a standard solution concentration of 1.4 ng mL<sup>-1</sup> for the labeled levoglucosan compound (<sup>13</sup>C<sub>6</sub> enriched to 98%, purity of 98%) and a concentration of 0.4 ng mL<sup>-1</sup> for the native levoglucosan (purity of 99.7%). Samples were prepared under a Class 100 clean bench in a Class 10,000 clean room by transferring 675 μL of the melted ice from the storage bottle and adding 25 μL (35 ng) of the labeled levoglucosan internal standard into the 700 μL pre-cleaned LDPE vials. Levoglucosan quantification was performed by Isotope Dilution Mass Spectrometry (IDMS) using labeled levoglucosan, and comparing the native compound peak

38 area with that of  $^{13}\text{C}_6$  isotopomer. Instrumental response factors were analysed before, during and at the end  
39 of each sample analysis set in order to evaluate instrumental response deviations. Response factors contained  
40 combined levoglucosan and  $^{13}\text{C}_6$ -labeled levoglucosan at a concentration of  $50 \text{ pg mL}^{-1}$  in ultrapure water.  
41 Chromatographic separations were conducted on an Agilent 1100 series liquid chromatography system  
42 (Agilent, Waldbronn, Germany). The HPLC system consists of a vacuum degasser unit, a binary pump,  
43 autosampler, and thermostatted column unit. Separation was performed injecting  $300 \mu\text{L}$  (LOOP Multidraw  
44 Upgrade Kit G1313 - 68711 for Agilent 1100 series autosampler) in a C18 Synergy Hydro column ( $4.6 \text{ mm}$   
45  $\text{i.d.} \times 50 \text{ mm}$  length,  $4 \mu\text{m}$  particle size, Phenomenex, Torrance, CA). For the off-line post column addition of  
46 the ammonium hydroxide solution we used a Waters 515 HPLC pump (Waters Corporation, Milford, MA).  
47 The mass analyser detector used to determine and quantify levoglucosan in Arctic ice was an API 4000 triple  
48 quadrupole mass spectrometer (Applied Biosystems/MDS SCIEX, Toronto, Ontario, Canada) equipped with  
49 Turbo V ion spray source (ESI). The ion source was operated in the negative mode and three characteristic  
50 transitions for levoglucosan and isotopic enriched internal standard were monitored by multiple reaction  
51 monitoring with a  $200 \text{ ms}$  dwell time/transition. The transitions  $161/113 \text{ m/z}$  for levoglucosan and  $167/118 \text{ m/z}$   
52 for labeled levoglucosan were used for the sample quantification.

53  
54

## 55 **DATA ANALYSIS AND VALIDATION**

56 NEEM levoglucosan concentrations varied from  $9 \text{ pg mL}^{-1}$  to  $1767 \text{ pg mL}^{-1}$ . The data exhibit high variance  
57 with abrupt changes between points, resulting in a high percentage variation coefficient (or relative standard  
58 deviation), defined as  $(\sigma/\bar{x}) \times 100$ , equal to  $167.4\%$ . Including all data results in mean of  $92 \text{ pg mL}^{-1}$  where  
59 most of samples ( $205/273$ ,  $75.1\%$ ) then become negative anomalies.

60

### 61 **Statistical analysis**

62 We calculated the correlation between the levoglucosan data and major ions measured by continuous flow  
63 analysis (CFA) at the NEEM camp. This correlation includes all available data (from  $98.45 \text{ m}$  to  $450.45 \text{ m}$ ,  
64 from AD 1657 to BCE 144) from the deep ice core. CFA major ion data are available for each  $55\text{-cm}$  bag, but  
65 the levoglucosan data are for two consecutive bags, or  $110\text{-cm}$  samples. We therefore calculated average values  
66 of the major ion data to correspond with the levoglucosan depths. If one variable (a major ion or levoglucosan)  
67 was not recorded over a  $110\text{-cm}$  interval, we did not include any of the other data over this interval. As BC  
68 was measured on a parallel core, and as BC data have much higher resolution, we do not include these data in  
69 our analysis in order to avoid error resulting in the attempt to calculate BC averages from NEEM-2011-S1  
70 core over the same temporal interval covered by the deep NEEM core.

71

72 We examined the normality of our dataset as well as the normality of each variable in order to determine if we  
73 should use the raw levoglucosan data or transformed (i.e. logarithmic) values. We applied a Shapiro-Wilk  
74 normality test and we also calculated skewness and kurtosis. Levoglucosan data distribution is asymmetric

75 rather than normal (Shapiro-Wilk normality test, p-value < 2.2 10<sup>-16</sup>), with a long upper tail resulting from few  
 76 strong levoglucosan spikes, yet it is not log-normally distributed. We can determine with an  $\alpha = 0.05$  that all  
 77 the variables are not normally distributed with exception of H<sub>2</sub>O<sub>2</sub>. This consideration is confirmed looking at  
 78 skewness and kurtosis values that are, respectively, -0.37 and kurtosis = 0.055 (it is known that a normal  
 79 distribution has kurtosis = 0). We then tested if our data (not including H<sub>2</sub>O<sub>2</sub>) are log-normally distributed.  
 80 After applying a log transformation to our original dataset, we reapplied the Shapiro-Wilk normality test. The  
 81 variables Ca<sup>2+</sup>, NH<sub>4</sub><sup>+</sup> and HCHO are log-normally distributed with  $\alpha = 0.05$ . Therefore we cannot assume a  
 82 normal distribution for our entire set of variables, even if they are log-transformed.

83  
 84 We then applied Pearson and Spearman correlations. The Pearson correlation is computed on *true values* and  
 85 benchmark linear relationships between variables. The Spearman correlation is a non-parametric analog and  
 86 is calculated on ranked data (Table S1). In a second step, in order to avoid a misleading interpretation of  
 87 correlation values, we decided not to include sulphate measurements as sulphate has a large number of missing  
 88 values (Table S2) that limit the amount of available data for calculating correlation.  
 89 In both cases (presence/absence of sulphate) levoglucosan does not correlate with the crustal markers Ca<sub>2</sub> and  
 90 dust, but does slightly correlate with ammonium (Table 1 and 2).

91  
 92 **Pearson correlation**

	Na <sup>+</sup>	Ca <sup>++</sup>	dust	NH <sub>4</sub> <sup>+</sup>	NO <sub>3</sub> <sup>-</sup>	SO <sub>4</sub> <sup>=</sup>	H <sub>2</sub> O <sub>2</sub>	HCOH	levo
Na <sup>+</sup>	1.00	0.11	0.06	0.01	0.10	-0.19	-0.12	0.03	-0.01
Ca <sup>++</sup>	0.11	1.00	0.04	0.06	0.02	-0.51	-0.13	0.17	-0.06
dust	0.06	0.04	1.00	0.00	0.16	-0.09	-0.03	0.04	0.02
NH <sub>4</sub> <sup>+</sup>	0.01	0.06	0.00	1.00	0.23	0.09	0.22	-0.01	0.42
NO <sub>3</sub> <sup>-</sup>	0.10	0.02	0.16	0.23	1.00	0.06	-0.09	0.06	0.02
SO <sub>4</sub> <sup>=</sup>	-0.19	-0.51	-0.09	0.09	0.06	1.00	0.24	-0.11	0.07
H <sub>2</sub> O <sub>2</sub>	-0.12	-0.13	-0.03	0.22	-0.09	0.24	1.00	0.01	0.06
HCOH	0.03	0.17	0.04	-0.01	0.06	-0.11	0.01	1.00	-0.02
levo	-0.01	<b>-0.06</b>	<b>0.02</b>	<b>0.42</b>	0.02	0.07	0.06	-0.02	1.00

93  
 94

95 **Spearman correlation**

	Na <sup>+</sup>	Ca <sup>++</sup>	dust	NH <sub>4</sub> <sup>+</sup>	NO <sub>3</sub> <sup>-</sup>	SO <sub>4</sub> <sup>=</sup>	H <sub>2</sub> O <sub>2</sub>	HCOH	levo
Na <sup>+</sup>	1.00	0.21	0.23	0.02	0.05	-0.21	-0.17	-0.01	-0.17
Ca <sup>++</sup>	0.21	1.00	0.39	0.06	0.03	-0.47	-0.22	0.22	-0.02
dust	0.23	0.39	1.00	0.06	0.16	-0.07	-0.11	0.06	-0.09
NH <sub>4</sub> <sup>+</sup>	0.02	0.06	0.06	1.00	0.21	0.13	0.27	0.14	0.45
NO <sub>3</sub> <sup>-</sup>	0.05	0.03	0.16	0.21	1.00	0.06	-0.07	0.09	0.03
SO <sub>4</sub> <sup>=</sup>	-0.21	-0.47	-0.07	0.13	0.06	1.00	0.17	-0.21	0.17
H <sub>2</sub> O <sub>2</sub>	-0.17	-0.22	-0.11	0.27	-0.07	0.17	1.00	0.03	0.20
HCOH	-0.01	0.22	0.06	0.14	0.09	-0.21	0.03	1.00	0.04
levo	-0.17	<b>-0.02</b>	<b>-0.09</b>	<b>0.45</b>	0.03	0.17	0.20	0.04	1.00

96

97 **Table S1** Pearson (above) and Spearman (bottom) correlation matrix of all data. Red numbers emphasize  
 98 correlations between levoglucosan and crustal markers Ca<sup>++</sup> and dust. Numbers in bold emphasize correlations  
 99 between levoglucosan and NH<sub>4</sub><sup>+</sup>.

100

101 **Pearson's correlation**

	Na <sup>+</sup>	Ca <sup>++</sup>	dust	NH <sub>4</sub> <sup>+</sup>	NO <sub>3</sub> <sup>-</sup>	H <sub>2</sub> O <sub>2</sub>	HCOH	levo
Na <sup>+</sup>	1.00	0.08	0.06	0.00	0.09	-0.13	0.01	-0.02
Ca <sup>++</sup>	0.08	1.00	0.02	0.05	0.00	-0.08	0.18	-0.05
dust	0.06	0.02	1.00	0.00	0.17	-0.03	0.05	0.02
NH <sub>4</sub> <sup>+</sup>	0.00	0.05	0.00	1.00	0.21	0.21	0.02	0.41
NO <sub>3</sub> <sup>-</sup>	0.09	0.00	0.17	0.21	1.00	-0.04	0.04	0.02
H <sub>2</sub> O <sub>2</sub>	-0.13	-0.08	-0.03	0.21	-0.04	1.00	-0.01	0.04
HCOH	0.01	0.18	0.05	0.02	0.04	-0.01	1.00	-0.03
levo	-0.02	<b>-0.05</b>	<b>0.02</b>	<b>0.41</b>	0.02	0.04	-0.03	1.00

102

103 **Spearman's correlation**

	Na <sup>+</sup>	Ca <sup>++</sup>	dust	NH <sub>4</sub> <sup>+</sup>	NO <sub>3</sub> <sup>-</sup>	H <sub>2</sub> O <sub>2</sub>	HCOH	levo
Na <sup>+</sup>	1.00	0.19	0.24	0.02	0.03	-0.19	0.00	-0.16
Ca <sup>++</sup>	0.19	1.00	0.34	0.07	0.02	-0.16	0.24	0.02
dust	0.24	0.34	1.00	0.10	0.18	-0.11	0.10	-0.06
NH <sub>4</sub> <sup>+</sup>	0.02	0.07	0.10	1.00	0.19	0.24	0.18	0.45
NO <sub>3</sub> <sup>-</sup>	0.03	0.02	0.18	0.19	1.00	-0.02	0.05	0.00
H <sub>2</sub> O <sub>2</sub>	-0.19	-0.16	-0.11	0.24	-0.02	1.00	0.02	0.18
HCOH	0.00	0.24	0.10	0.18	0.05	0.02	1.00	0.05
levo	-0.16	<b>0.02</b>	<b>-0.06</b>	<b>0.45</b>	0.00	0.18	0.05	1.00

104

105 **Table S2** Pearson (above) and Spearman (bottom) correlation matrix of all data without sulphate. Red numbers  
106 emphasize correlations between levoglucosan and crustal markers  $\text{Ca}^{++}$  and dust. Numbers in bold emphasize  
107 correlations between levoglucosan and  $\text{NH}_4^+$ .

108

### 109 **Smoothing analysis and the Global Charcoal Database (GCD) record**

110 We tested different approaches in order to determine multi-decadal fire activity from levoglucosan  
111 concentrations. In order to compare levoglucosan data with decadal to centennial trends in other paleoclimate  
112 records, we first applied standardized statistical procedures based on those used to analyze the Global Charcoal  
113 Database (GCD) (Marlon et al., 2008; Power et al., 2008), which is a robust method for summarizing different  
114 datasets from various environmental archives. These techniques are described in detail elsewhere (Marlon et  
115 al., 2008; Power et al., 2008), where the procedure is summarized with the following steps:

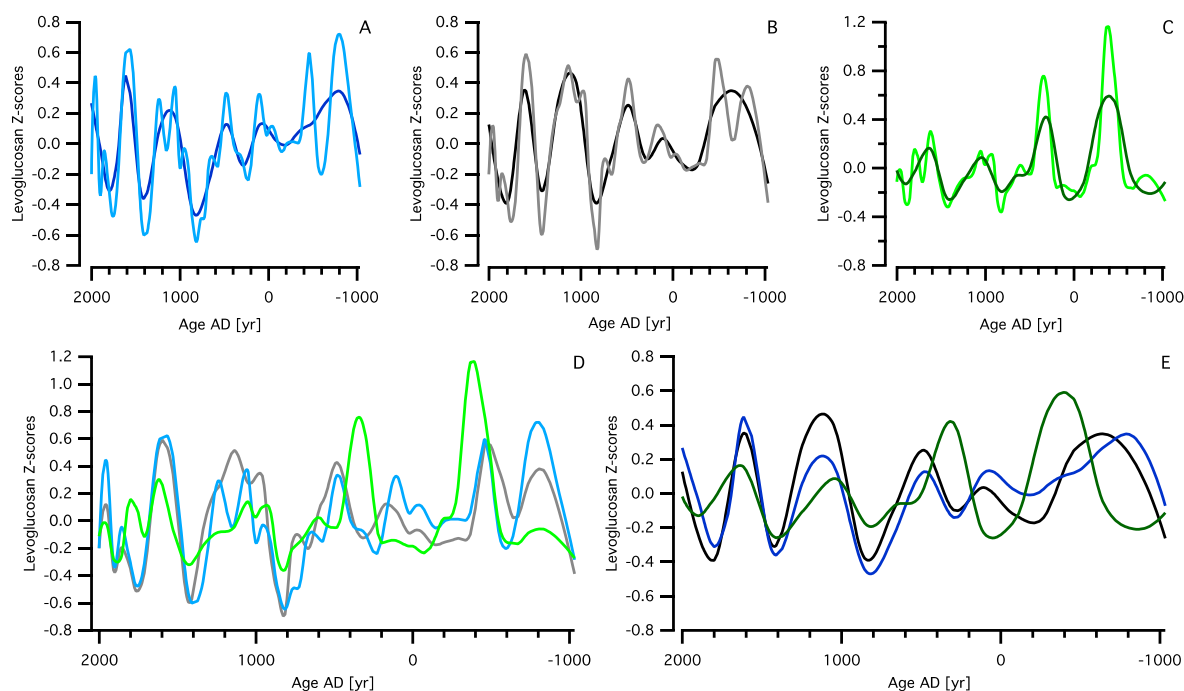
- 116 a) Box Cox transformation to homogenize variance of the record.
- 117 b) Mini-max transformation to rescale data to a range between 0 and 1
- 118 c) Z-score with standard deviation and mean calculated over the period AD 1000 - 1800
- 119 d) APPROX package for R software (linear interpolation that creates output data equally spaced over time)
- 120 e) LOWESS (Locally Weighted Scatterplot Smoothing) model (Cleveland and Grosse, 1991).

121 This approach minimizes the influence of outliers, which helps filter noise from the data. It uses every data  
122 point, including anomalous values.

123

124 We differ from the GCD procedure in our treatment of individual spikes, as these strongly affect multi-decadal  
125 trends, even when using a LOWESS regression model. As shown in Fig. S1 C, century-long peaks were  
126 generated by single levoglucosan spikes, i.e. around AD 340. The centennial peak was an artifact since it is  
127 produced by only one sample with a high levoglucosan concentration in a period of unexceptional fire activity.  
128 We examined other solutions to solve the “smoothing problem” (i.e. use of pre-smoothing, median-based  
129 approach) but we preferred avoiding further approximation of the real behavior of levoglucosan  
130 concentrations. In order to minimize the influence of high levoglucosan spikes on the general trend, we applied  
131 LOWESS to our data after omitting peaks above a fixed threshold (Fig. S1). Excluded peaks were studied  
132 separately. Using suggestions in the literature (Tukey, 1977), we selected the following threshold:  $3rd\_Q +$   
133  $1.5 \times IR$ , which corresponds to a concentration of  $168 \text{ pg mL}^{-1}$  in our NEEM levoglucosan record.  $3rd\_Q$  is  
134 the third quartile and  $IR$  is the interquartile range calculated as the difference between the third quartile and  
135 the first quartile (Fig. S1 A).

136



137

138 **Fig. S1** Effect of levoglucosan spikes. LOWESS smoothing with SPAN parameter (f) 0.1 (light blue) and 0.2  
 139 (blue) of levoglucosan Z-scores without peaks above the threshold  $3rd\_Q + 1.5 \times IR$  (where  $3rd\_Q$  is the third  
 140 quartile and  $IR$  is the interquartile range calculated as the difference between the third quartile and the first  
 141 quartile) (A); same transformation of A but using the threshold  $\bar{x} + \sigma$ , with  $f = 0.1$  (gray) and  $f = 0.2$  (black)  
 142 (B); LOWESS smoothing including spikes with SPAN parameter (f) 0.1 (light green) and 0.2 (green) (C);  
 143 comparison between LOWESS with  $f = 0.1$  presented in A (light blue), B (gray) and C (light green) (D);  
 144 comparison between LOWESS with  $f = 0.2$  presented in A (blue), B (black) and C (green) (E).

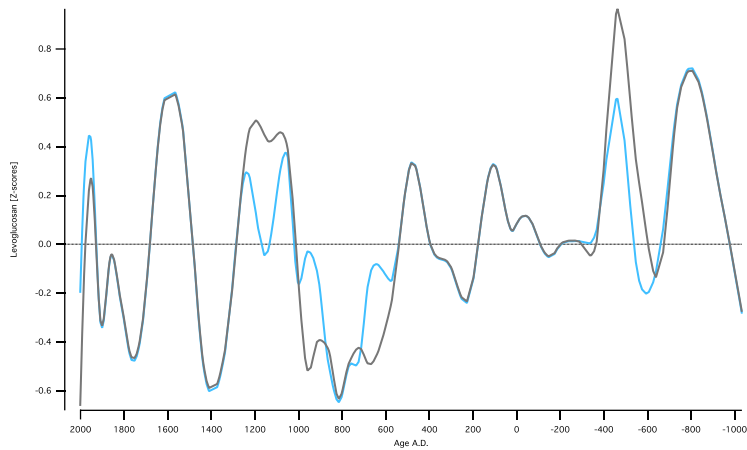
145

146 One of the intrinsic problems of ice core analyses is that the samples are often equidistant in depth, but not  
 147 equidistant in time. We tried using statistics to create data output that is equally spaced over time. However  
 148 statistical interpolations (linear or other) generate “unreal” data during periods not covered by the analyses.  
 149 The quality of the final smoothed function becomes less reliable, in the sense that the final smoothed data are  
 150 less similar to the measured data. We hesitate to apply this technique as this approach results in data that are  
 151 only interpolated rather than actually measured, and the resulting smoothed data set is yet another step farther  
 152 away from the measured values.

153 We tested using a moving window for the definition of thresholds. We divided the whole dataset in ten subsets,  
 154 where each subset had 10% of the data. We decided to fix the amount of data in each subset to guarantee the  
 155 possibility to calculate significant statistical indicators (i.e. mean, deviation standard, etc.). We calculated the  
 156 threshold (the  $3rdQ + 1.5IR$ ) and we individuated the outliers for each subset. Using the fixed threshold results  
 157 in 24 outliers, while using a moving window results in 25. Of the outliers identified by the moving window,  
 158 22 of these are the same as the 24 outliers using the fixed threshold.

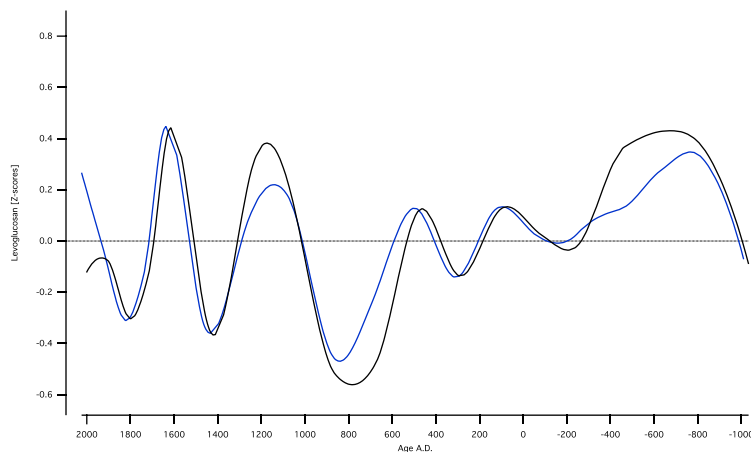
159 We compare the smoothed data after the outliers were removed using the two methods in Figures S2 and S3.  
 160 No major differences occur from using the different threshold calculation forms.

161



162

163 **Fig. S2** Effect of different threshold calculations. LOWESS smoothing with SPAN parameter (f) 0.1 of  
 164 levoglucosan Z-scores without peaks above the fixed threshold  $3rd\_Q + 1.5 \times IR$  (where  $3rd\_Q$  is the third  
 165 quartile and  $IR$  is the interquartile range calculates as the difference between the third quartile and the first  
 166 quartile) (light blue); LOWESS smoothing with SPAN parameter (f) 0.1 of levoglucosan Z-scores without  
 167 peaks above the thresholds  $3rd\_Q + 1.5 \times IR$  calculated in ten subsets, each one containing 10% of data (gray).  
 168



169

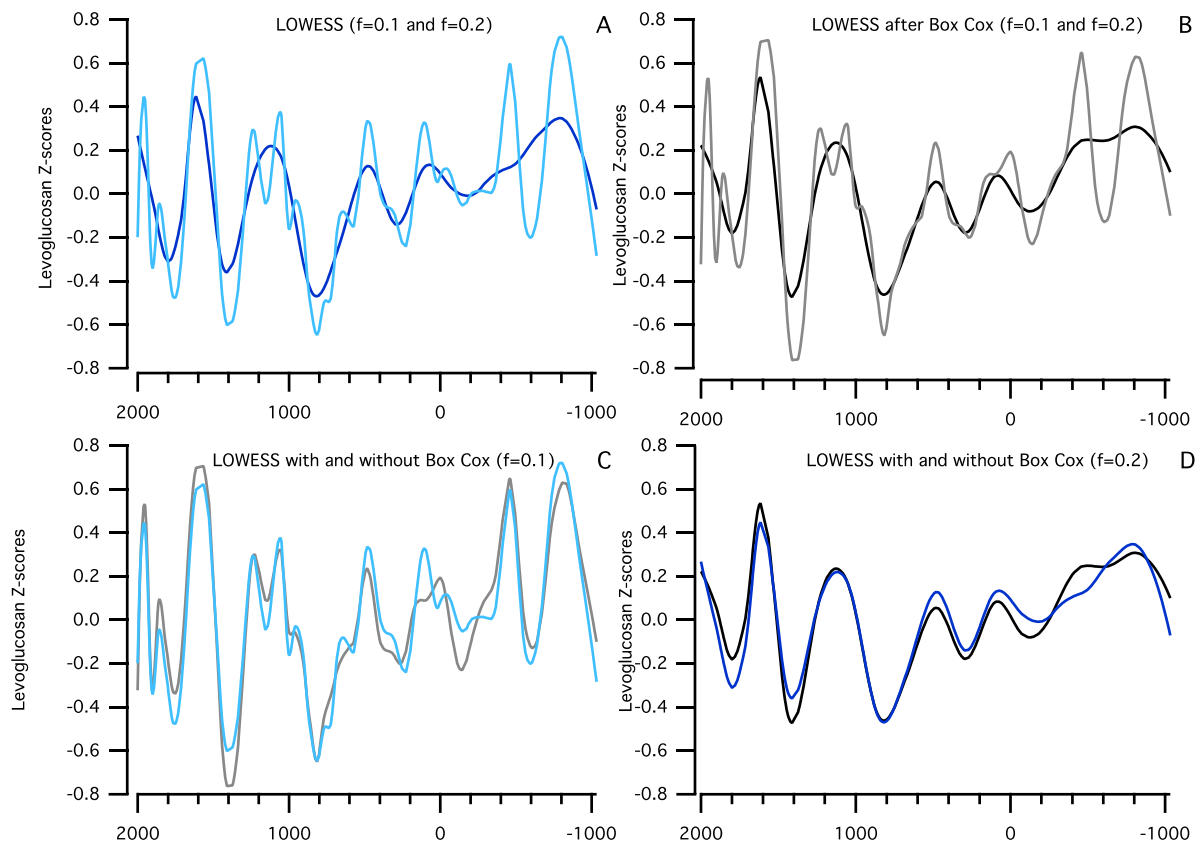
170 **Fig. S3** LOWESS smoothing with SPAN parameter (f) 0.2 of levoglucosan Z-scores without peaks above the  
 171 fixed threshold  $3rd\_Q + 1.5 \times IR$  (where  $3rd\_Q$  is the third quartile and  $IR$  is the interquartile range calculates  
 172 as the difference between the third quartile and the first quartile) (blue); LOWESS smoothing with SPAN  
 173 parameter (f) 0.2 of levoglucosan Z-scores without peaks above the thresholds  $3rd\_Q + 1.5 \times IR$  calculated in  
 174 ten subsets, each one containing 10% of data (black).  
 175

176

177 We tested the effect of the Box Cox transformation by observing the LOWESS results after applying a Box  
 178 Cox transformation on the levoglucosan dataset. The results from this comparison of statistical techniques  
 179 demonstrate that the Box Cox transformation does not appear to change the data distribution. Since the Box-  
 180 Cox transformation is not necessary (Fig. S4), as we have a single dataset, we prefer to avoid this additional  
 181 transformation on our data.

182





183

184 **Figure S4** Effect of Box Cox Transformation. LOWESS smoothing with SPAN parameter ( $f$ ) 0.1 (light blue)  
 185 and 0.2 (blue) of levoglucosan Z-scores without peaks above the threshold  $3rd\_Q + 1.5 \times IR$  (where  $3rd\_Q$   
 186 is the third quartile and  $IR$  is the interquartile range calculates as the difference between the third quartile  
 187 and the first quartile) (A); same transformation of A but with Box Cox transformation with  $f = 0.1$  (gray) and  $f =$   
 188  $0.2$  (black) (B); comparison between LOWESS with  $f = 0.1$  with Box Cox transformation (gray) and without  
 189 Box Cox transformation (light blue) (C); comparison between LOWESS with  $f = 0.2$  with Box Cox  
 190 transformation (black) and without Box Cox transformation (blue) (D).

191

192 Using the linear interpolation APPROX to obtain equally spaced data strongly influences the multi-decadal  
 193 trends and we prefer to use the original data rather than interpolated points.

194

195 In this work we used the following steps/approach:

- 196 a) Isolation of “outliers”
- 197 b) Z-score with standard deviation and mean calculated over the entire period covered by the dataset
- 198 c) Linear locally weighted polynomial regression model with tricube weight function commonly called  
 199 LOESS, the later generalization of LOWESS.

200 The smoothing parameter ( $\alpha$  or SPAN) is set to 0.1 and 0.2. These values give a nearest-neighbor based  
 201 bandwidth covering 10% and 20% of the data.

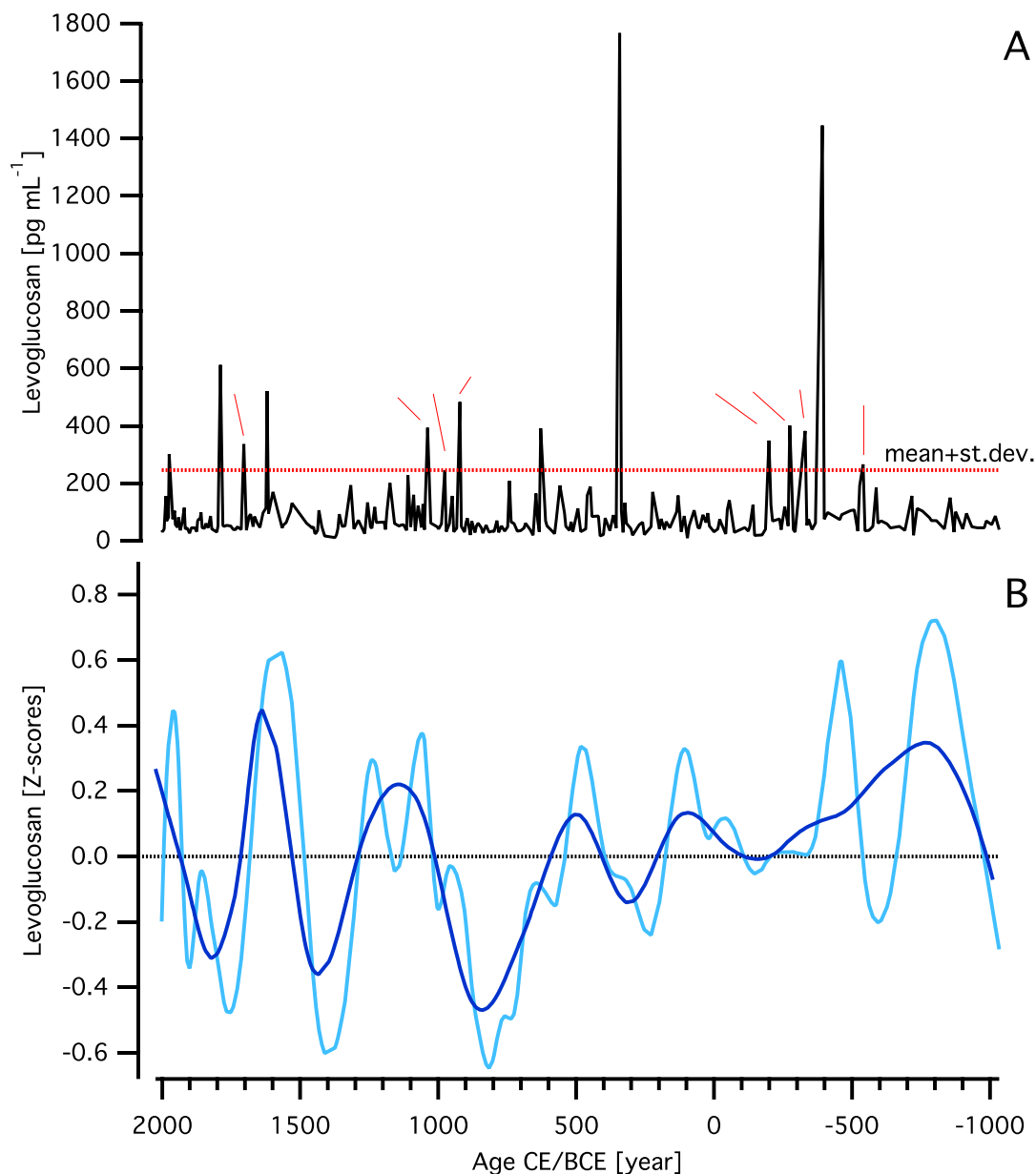
202 In order to compare the high-resolution BC records with the long-trend levoglucosan profile, we applied the

203 same statistical treatments as we used for the levoglucosan record. Ammonium has multiple anthropogenic  
204 and natural sources, and background values are linked to temperature changes (Fuhrer et al., 1993; Fuhrer et  
205 al., 1996; Legrand et al., 1992). Individual ammonium peaks correspond with levoglucosan peaks (Fig. 2,  
206 Table 1), but due to the incorporation of multiple sources in the ammonium record, we do not compare multi-  
207 decadal ammonium variability to the smoothed levoglucosan record.

208

## 209 MEGAFIRES

210

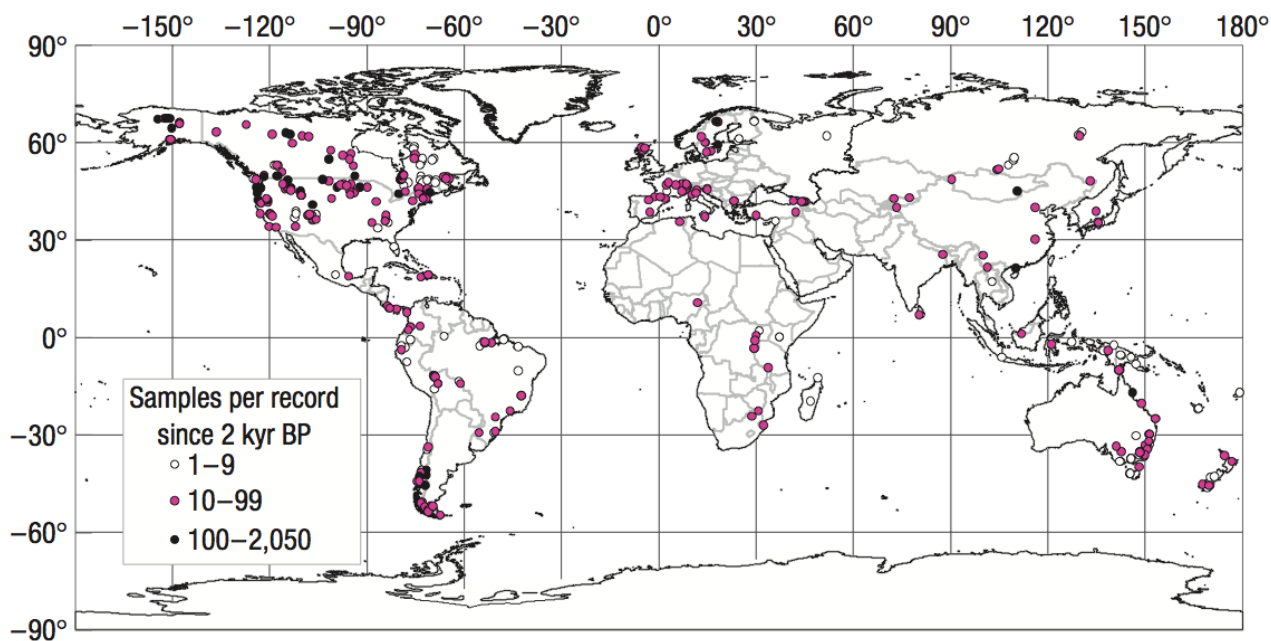


211

212 **Figure S5** Levoglucosan concentration profile and megafires (peaks with concentration above the average  
213 plus one standard deviation) (A); LOWESS smoothing with SPAN parameter (f) 0.1 (light blue) and 0.2 (blue)  
214 of levoglucosan Z-scores without peaks above the threshold  $3rd\_Q + 1.5 \times IR$  (where  $3rd\_Q$  is the third quartile  
215 and  $IR$  is the interquartile range calculated as the difference between the third quartile and the first quartile)  
216 (B).

217 THE GCD SAMPLING SITES

218

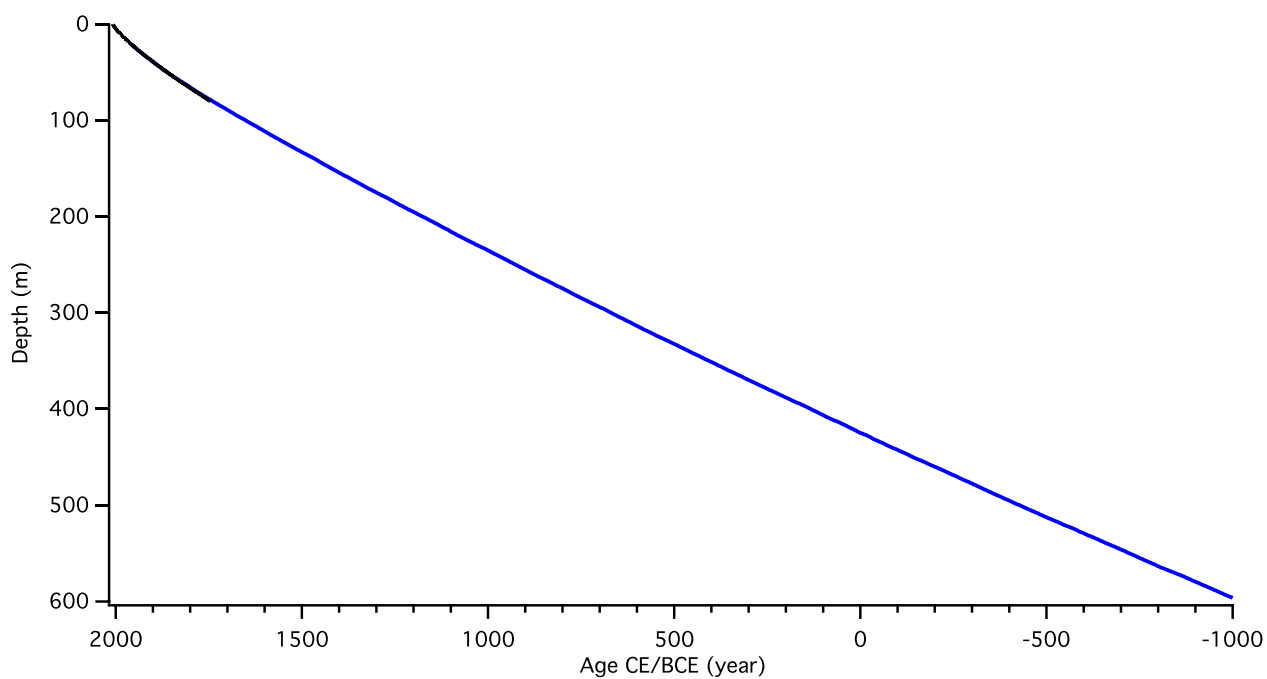


219

220 **Figure S6** Locations of charcoal records and samples number. Extracted from Marlon (2008).

221

222



223

224 **Figure S7** Age model representation. Blue points indicate the age-depth scale, as published in Rasmussen et  
225 al. (2013), black points are from the Herron-Langway firn densification model fit to the NEEM-NGRIP tie  
226 points for the 20-80 m long firn column.

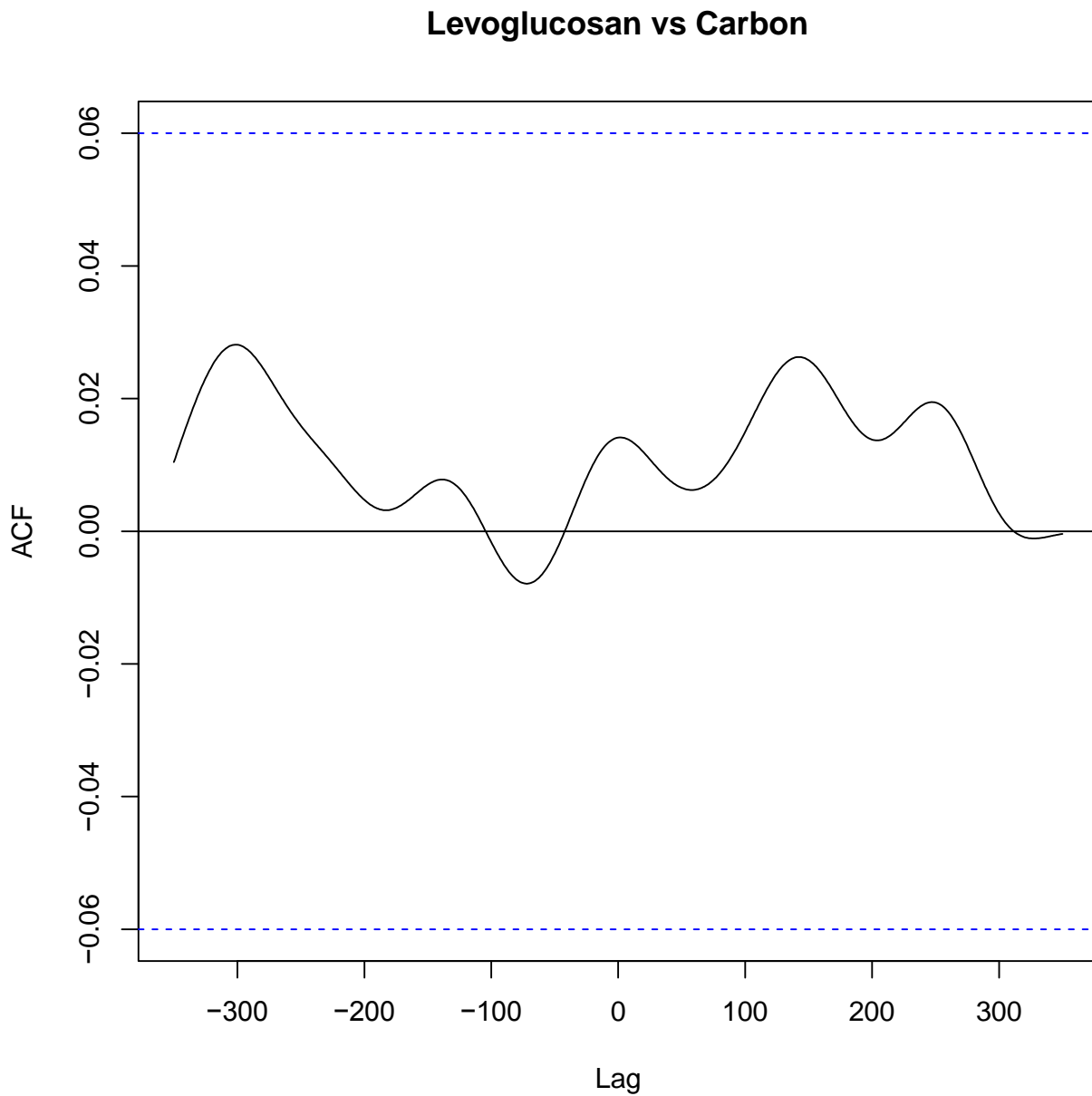
227

228 **Correlation Analyses**

229

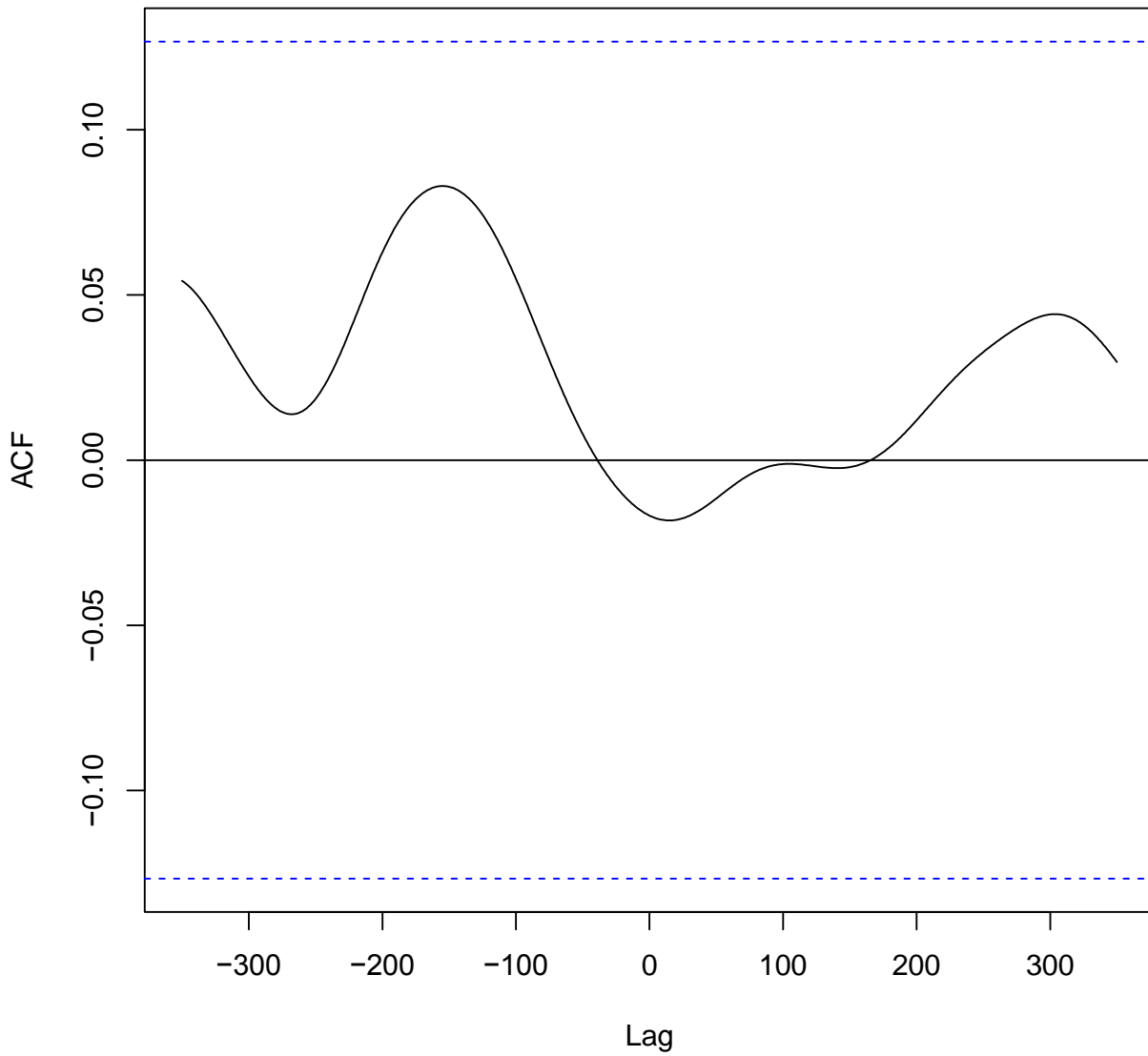
230 *Cross correlation between different time series*

231



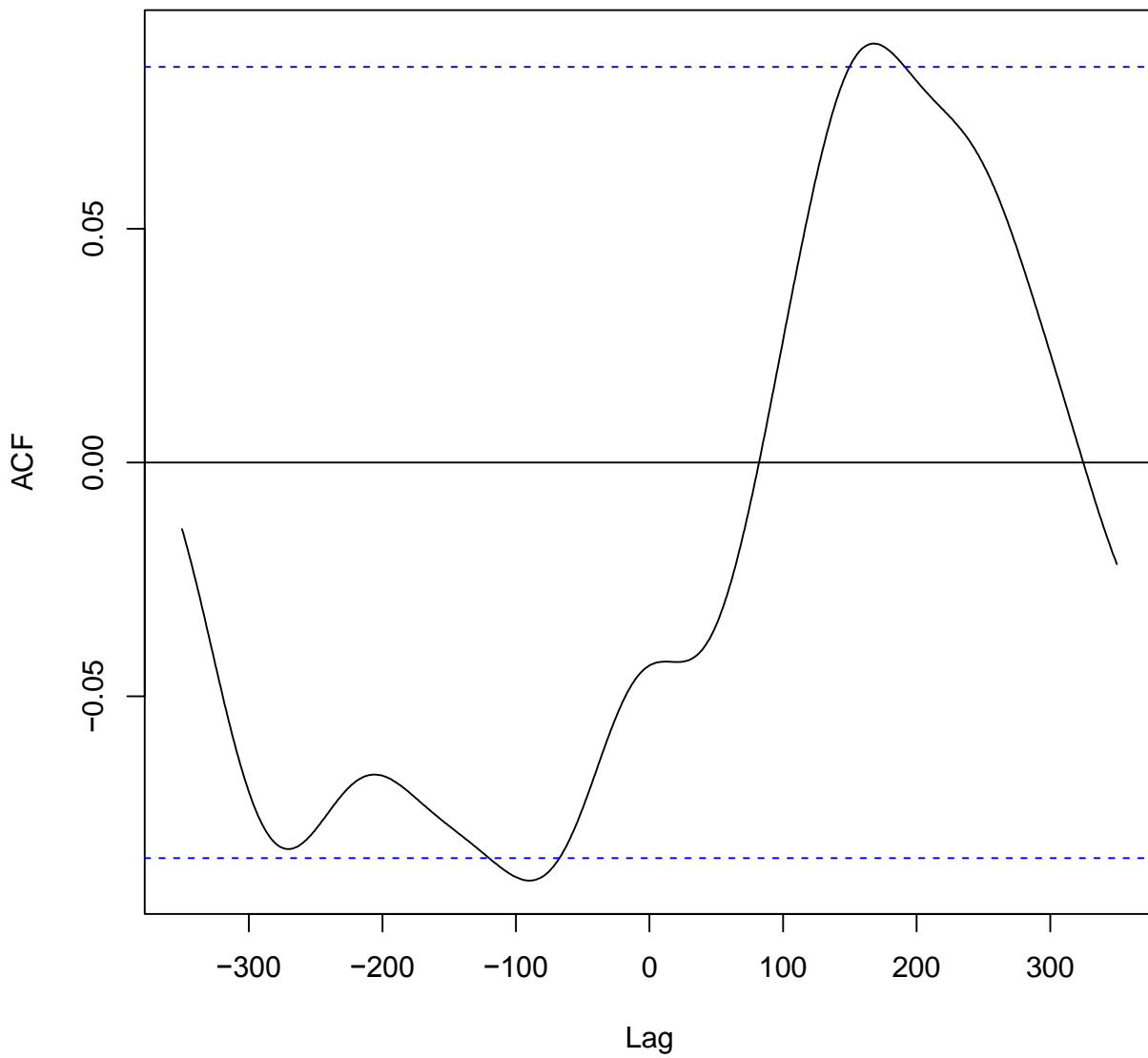
232 **Fig. S8** Cross correlation between levoglucosan and NEEM black carbon.  
233

### Levoglucosan vs Charcoal



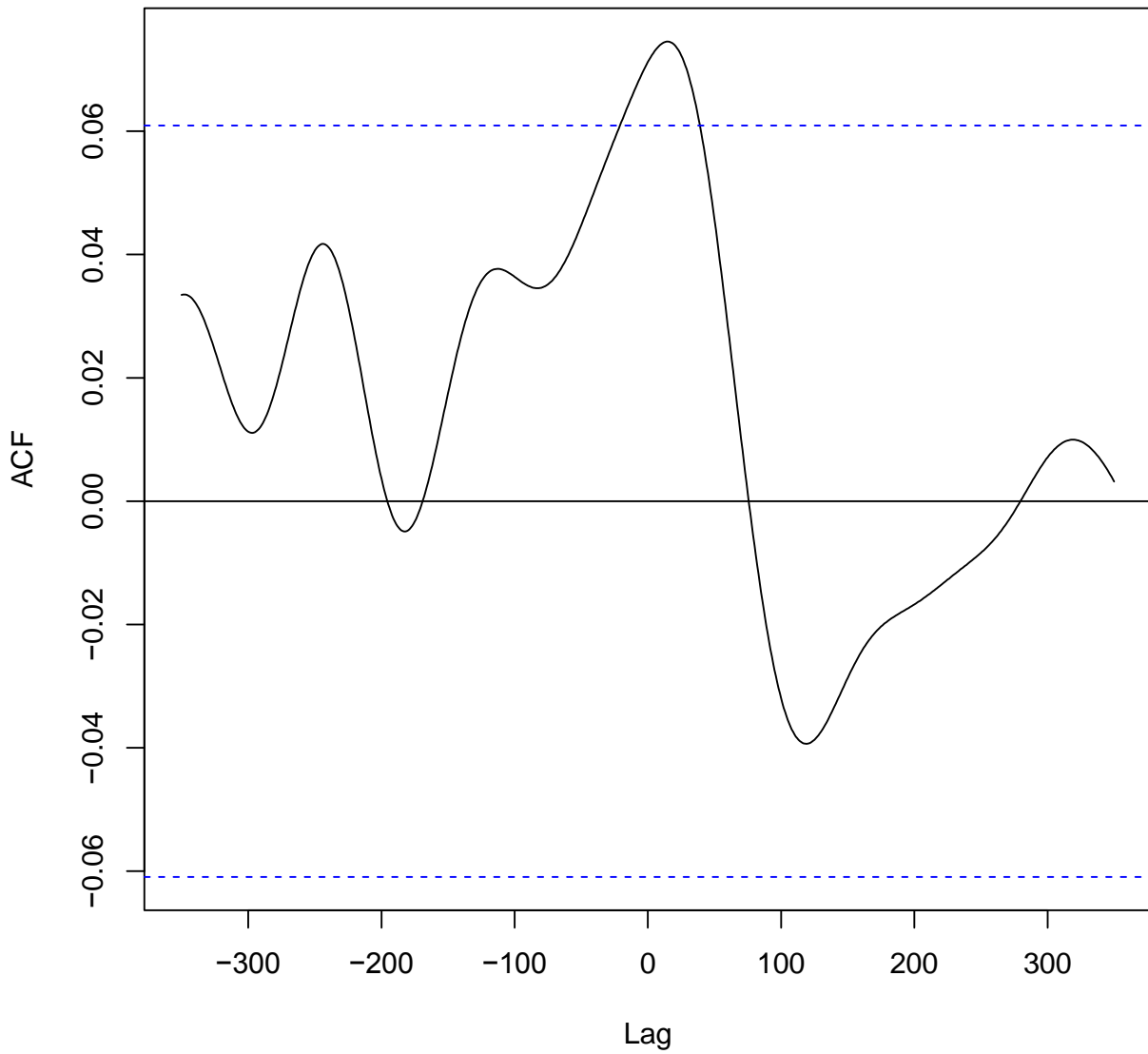
234  
235 **Fig. S9** Cross correlation between levoglucosan and high latitude (north of 55 °N) Northern  
236 Hemisphere charcoal synthesis.

### Levoglucosan vs Methane



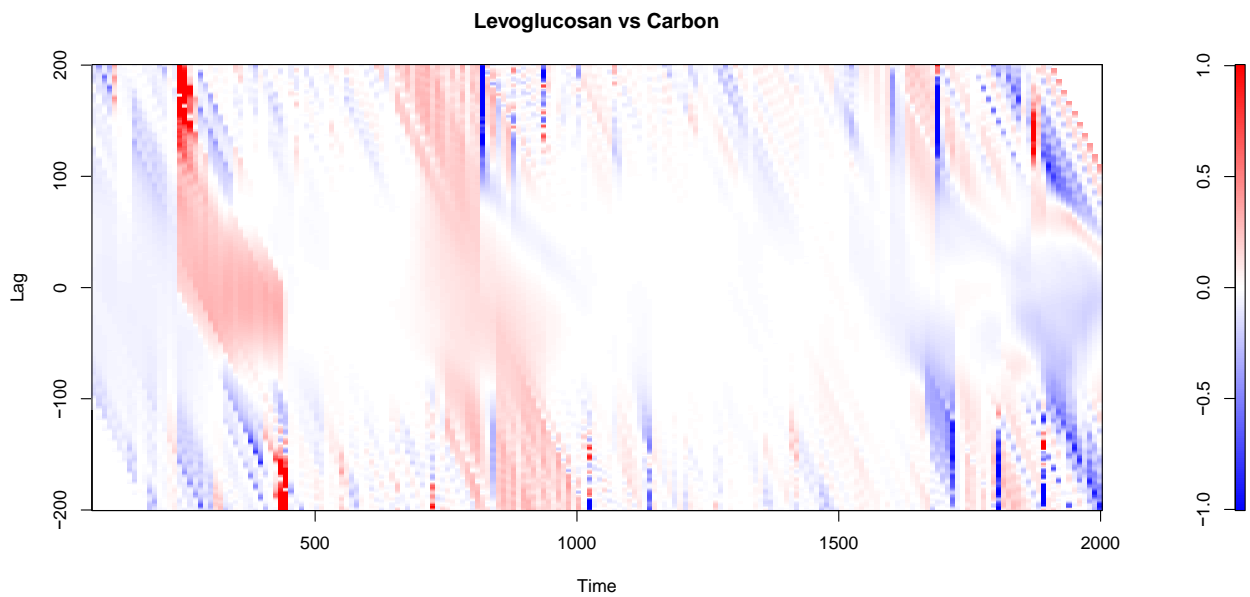
237  
238 **Fig. S10** Cross correlation between levoglucosan and atmospheric NEEM pyrogenic methane.

### Levoglucosan vs Temperature

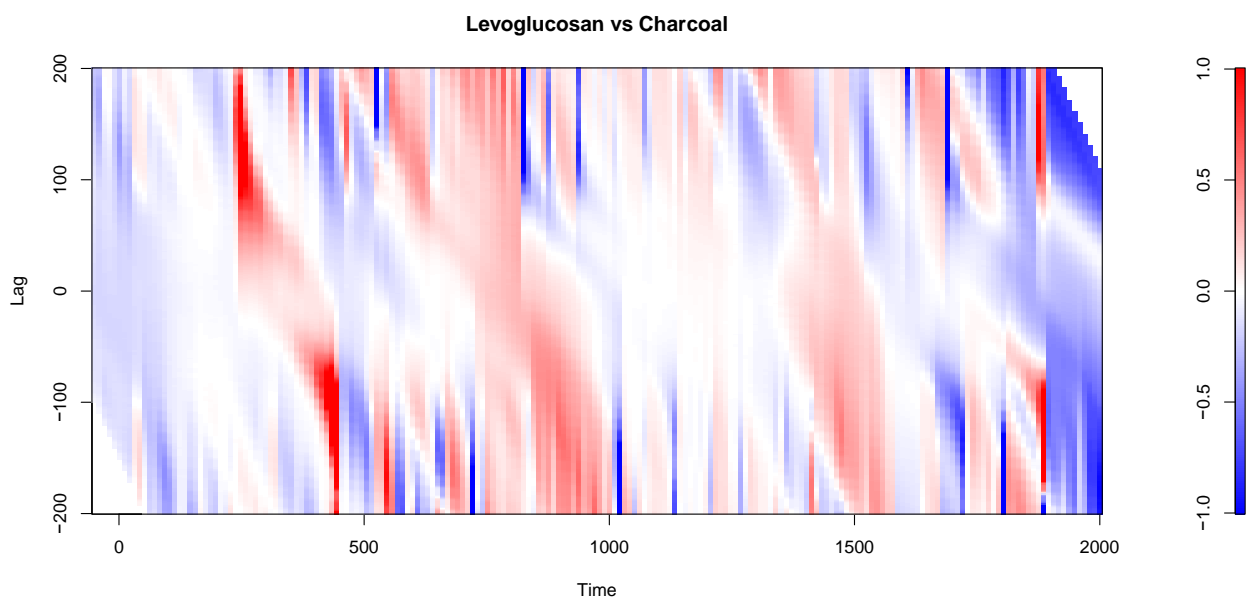


239  
240 **Fig. S11** Cross correlation between levoglucosan and Northern Hemisphere land temperature.  
241

242 *Local cross correlation between different time series*  
243

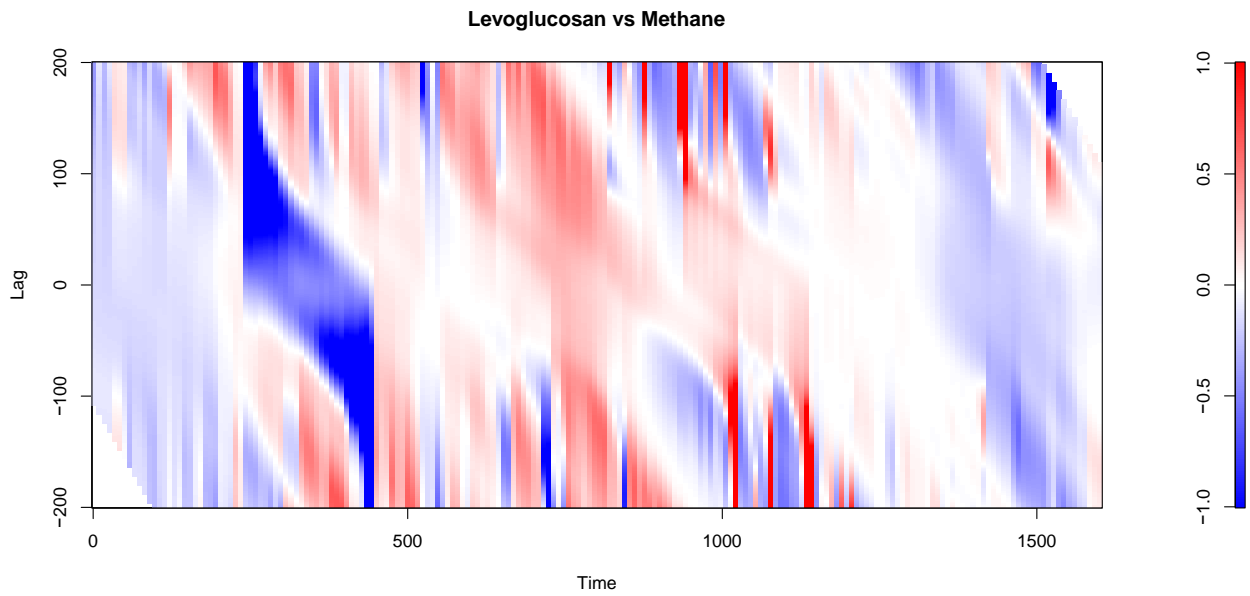


244 **Fig. S12** Local cross correlation between levoglucosan and NEEM black carbon  
245  
246  
247  
248

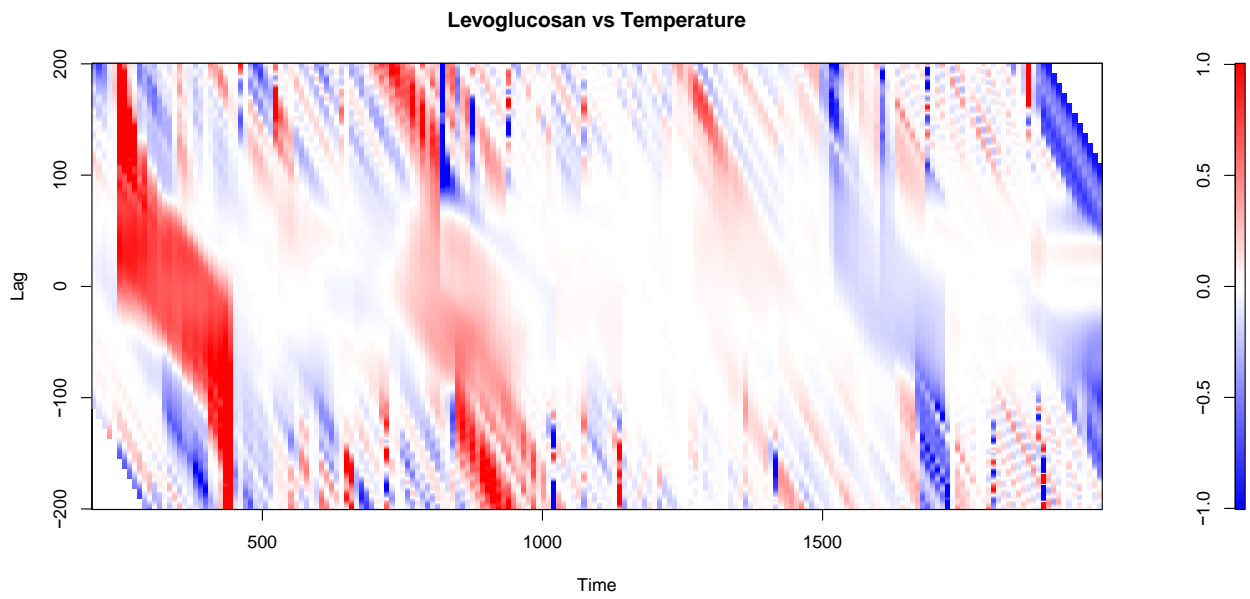


249 **Fig. S13** Local cross correlation between levoglucosan and high latitude (north of 55 °N) Northern  
250 Hemisphere charcoal synthesis.  
251  
252  
253





254  
 255 **Fig. S14** Local cross correlation between levoglucosan and NEEM pyrogenic methane.  
 256  
 257  
 258



259  
 260 **Fig. S15** Local cross correlation between levoglucosan and Northern Hemisphere land temperature  
 261  
 262

263 **References**

264

- 265 Barbante, C., Cozzi, G., Capodaglio, G., Van de Velde, K., Ferrari, C., Veysseyre, A., Boutron, C. F., Scarponi, G., and  
 266 Cescon, P.: Determination of Rh, Pd, and Pt in polar and alpine snow and ice by double focusing ICPMS with  
 267 microconcentric nebulization, *Anal. Chem.*, 71, 4125-4133, 10.1021/ac981437g, 1999.
- 268 Cleveland, W., and Grosse, E.: Computational methods for local regression, *Stat Comput*, 1, 47-62, 10.1007/bf01890836,  
 269 1991.
- 270 Fuhrer, K., Neftel, A., Anklin, M., and Maggi, V.: continuous measurements of hydrogen-peroxide, formaldehyde,  
 271 calcium and ammonium concentrations along the new grip ice core from summit, central greenland, *Atmospheric*  
 272 *Environment Part a-General Topics*, 27, 1873-1880, 10.1016/0960-1686(93)90292-7, 1993.
- 273 Fuhrer, K., Neftel, A., Anklin, M., Staffelbach, T., and Legrand, M.: High-resolution ammonium ice core record covering  
 274 a complete glacial-interglacial cycle, *J. Geophys. Res.-Atmos.*, 101, 4147-4164, 1996.
- 275 Gambaro, A., Zangrando, R., Gabrielli, P., Barbante, C., and Cescon, P.: Direct determination of levoglucosan at the  
 276 picogram per milliliter level in Antarctic ice by high-performance liquid chromatography/electrospray ionization triple  
 277 quadrupole mass spectrometry, *Anal. Chem.*, 80, 1649-1655, 10.1021/ac701655x, 2008.
- 278 Legrand, M., Deangelis, M., Staffelbach, T., Neftel, A., and Stauffer, B.: Large perturbation of ammonium and organic-  
 279 acids content in the Summit-Greenland ice core - Fingerprint from forest-fires, *Geophys. Res. Lett.*, 19, 473-475,  
 280 1992.
- 281 Marlon, J. R., Bartlein, P. J., Carcaillet, C., Gavin, D. G., Harrison, S. P., Higuera, P. E., Joos, F., Power, M. J., and  
 282 Prentice, I. C.: Climate and human influences on global biomass burning over the past two millennia, *Nat. Geosci.*, 1,  
 283 697-702, 10.1038/ngeo313, 2008.
- 284 Power, M. J., Marlon, J., Ortiz, N., Bartlein, P. J., Harrison, S. P., Mayle, F. E., Ballouche, A., Bradshaw, R. H. W.,  
 285 Carcaillet, C., Cordova, C., Mooney, S., Moreno, P. I., Prentice, I. C., Thonicke, K., Tinner, W., Whitlock, C., Zhang,  
 286 Y., Zhao, Y., Ali, A. A., Anderson, R. S., Beer, R., Behling, H., Briles, C., Brown, K. J., Brunelle, A., Bush, M.,  
 287 Camill, P., Chu, G. Q., Clark, J., Colombaroli, D., Connor, S., Daniau, A. L., Daniels, M., Dodson, J., Doughty, E.,  
 288 Edwards, M. E., Finsinger, W., Foster, D., Frechette, J., Gaillard, M. J., Gavin, D. G., Gobet, E., Haberle, S., Hallett,  
 289 D. J., Higuera, P., Hope, G., Horn, S., Inoue, J., Kaltenrieder, P., Kennedy, L., Kong, Z. C., Larsen, C., Long, C. J.,  
 290 Lynch, J., Lynch, E. A., McGlone, M., Meeks, S., Mensing, S., Meyer, G., Minckley, T., Mohr, J., Nelson, D. M.,  
 291 New, J., Newnham, R., Noti, R., Oswald, W., Pierce, J., Richard, P. J. H., Rowe, C., Goni, M. F. S., Shuman, B. N.,  
 292 Takahara, H., Toney, J., Turney, C., Urrego-Sanchez, D. H., Umbanhowar, C., Vandergoes, M., Vanniere, B.,  
 293 Vescovi, E., Walsh, M., Wang, X., Williams, N., Wilmshurst, J., and Zhang, J. H.: Changes in fire regimes since the  
 294 Last Glacial Maximum: an assessment based on a global synthesis and analysis of charcoal data, *Clim. Dyn.*, 30, 887-  
 295 907, 10.1007/s00382-007-0334-x, 2008.
- 296 Rasmussen, S. O., Abbott, P., Blunier, T., Bourne, A., Brook, E., Buchardt, S. L., Buizert, C., Chappellaz, J., Clausen, H.  
 297 B., Cook, E., Dahl-Jensen, D., Davies, S., Guillevic, M., Kipfstuhl, S., Laepple, T., Seierstad, I. K., Severinghaus, J.  
 298 P., Steffensen, J. P., Stowasser, C., Svensson, A., Vallelonga, P., Vinther, B. M., Wilhelms, F., and Winstrup, M.: A  
 299 first chronology for the NEEM ice core, *Clim. Past Discuss.*, 9, 2967-3013, 10.5194/cpd-9-2967-2013, 2013.
- 300 Tukey, J. W.: *Exploratory Data Analysis*, Addison-Wesley, 1977.

301

302